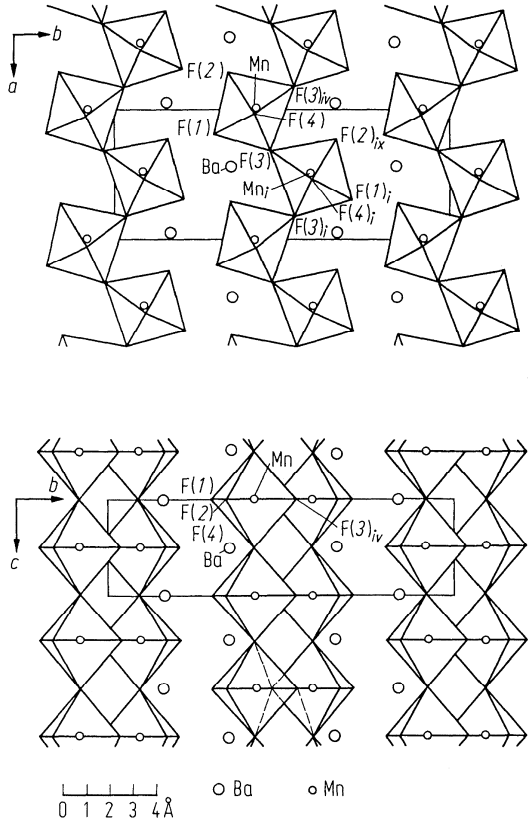

Fig. 26A-2-001. $BaMnF_4$. Crystal structure [69Kev]. Schematic view showing MnF_6 octahedra in $BaMnF_4$ structure along the *c* axis (upper) and along the *a* axis (lower). Subscripts attached to names of atoms denote symmetry operations. See Table 26A-2-006 about the nomenclature.

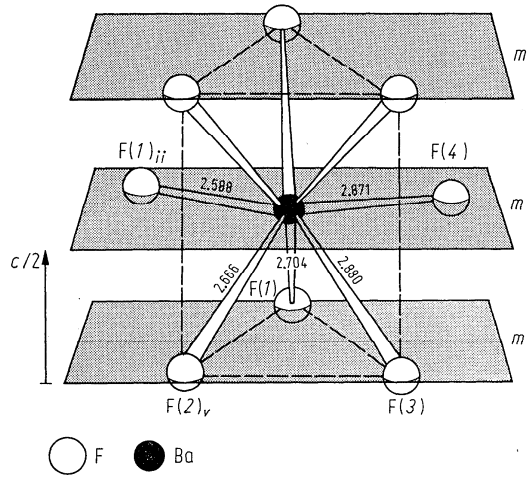

Fig. 26A-2-002. $BaMnF_4$. Crystal structure [69Kev]. Coordination polyhedron of fluorine atoms around Ba. Distances are in Å units and subscripts attached to names of atoms denote symmetry operations; for the explanation of the nomenclature, see Table 26A-2-006.

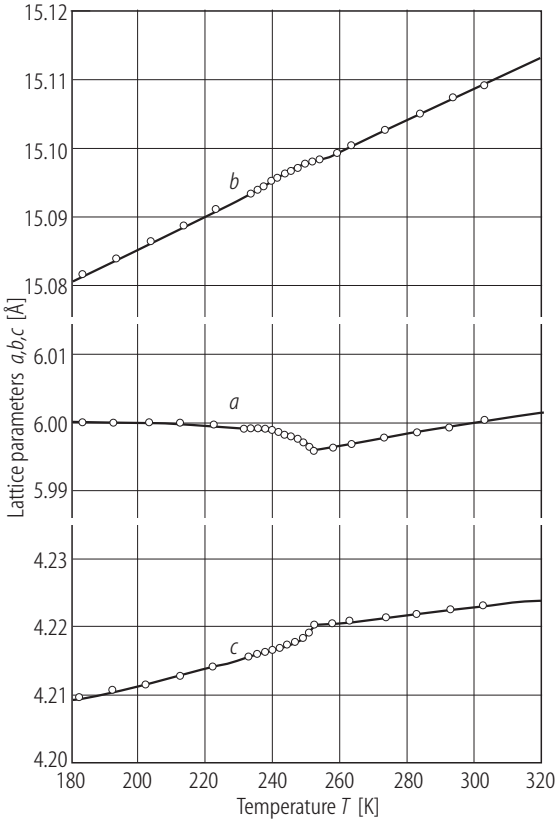

Fig. 26A-2-003. $BaMnF_4$. a, b, c vs. T [90Oga].

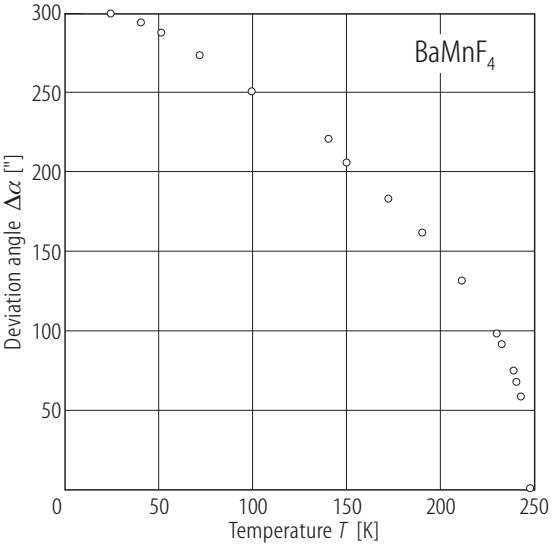

Fig. 26A-2-004. $BaMnF_4$. $\Delta\alpha$ vs. T [86StG]. $\Delta\alpha$: deviation angle of α from 90° estimated by the use of the splitting of (002) peaks.

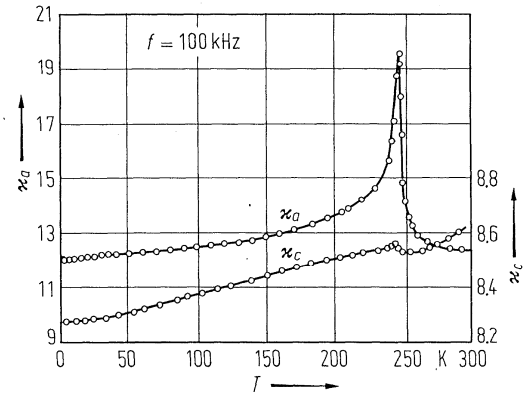

Fig. 26A-2-005. $BaMnF_4$. κ_a, κ_c vs. T [76Sam].

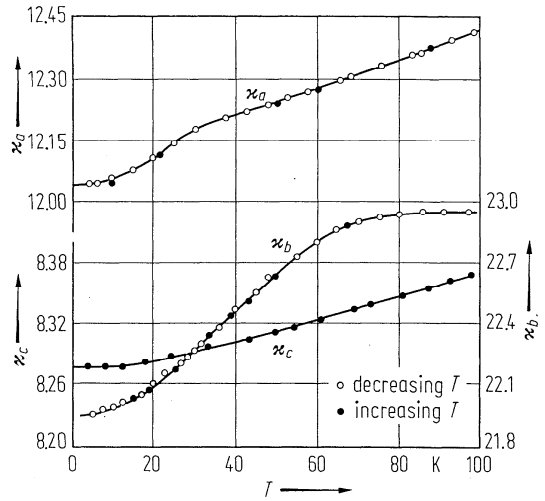

Fig. 26A-2-006. $BaMnF_4$. κ_a, κ_b, κ_c vs. T in low temperature region [77Sam]. f = 10…100 kHz.

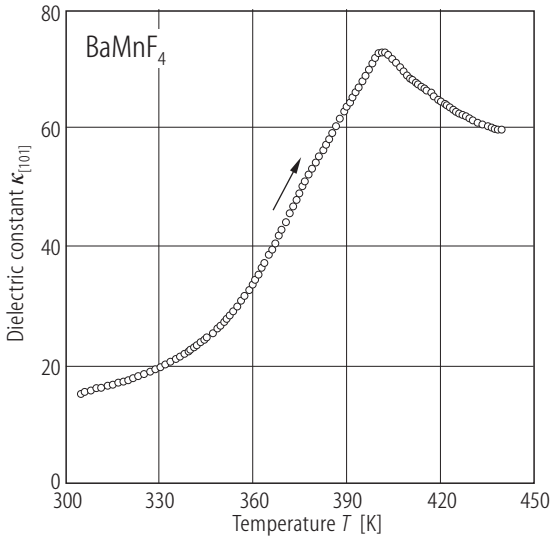

Fig. 26A-2-007. $BaMnF_4$. $\kappa_{[101]}$ vs. T [83Yos, 89Sco]. f = 100 kHz.

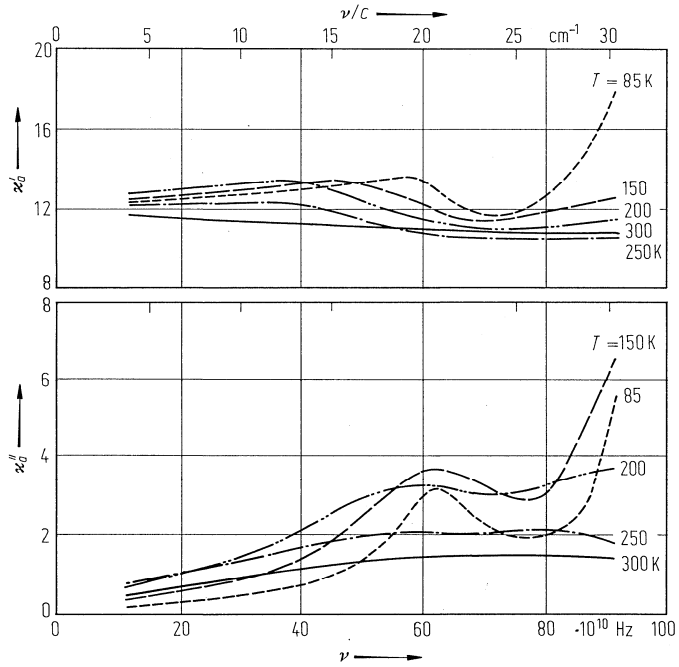

Fig. 26A-2-008. $BaMnF_4$. κ'_a, κ''_a vs. ν in a submillimeter range [82Vol]. Parameter: T.

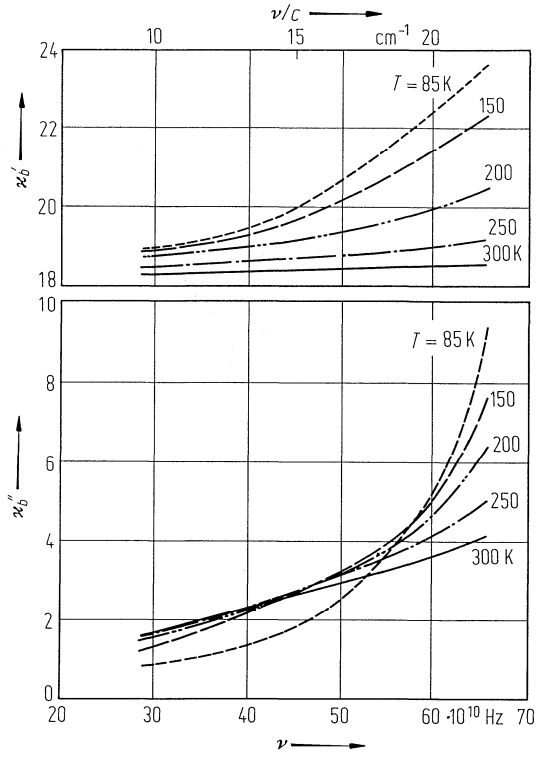

Fig. 26A-2-009. $BaMnF_4$. κ'_b, κ''_b vs. ν in a submillimeter range [82Vol]. Parameter: T.

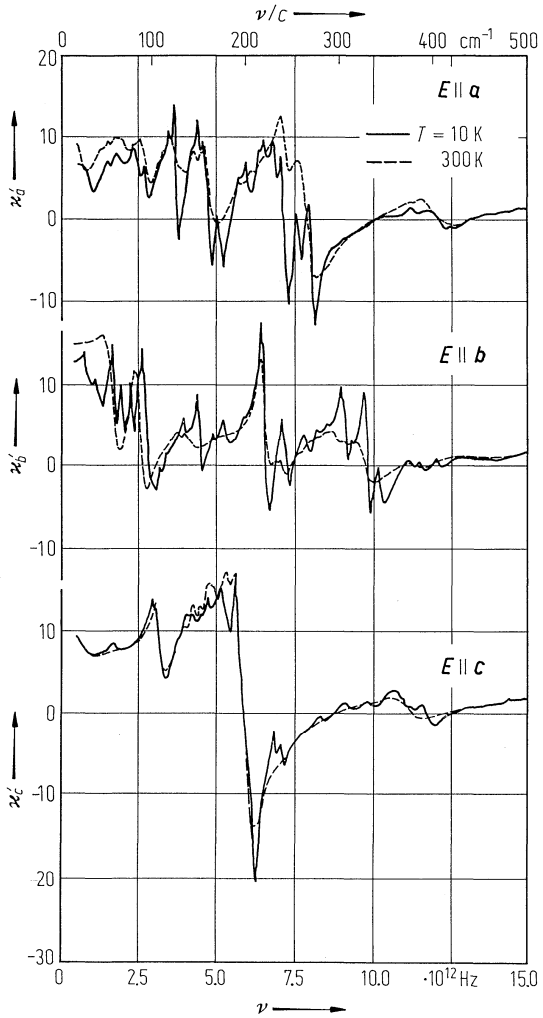

Fig. 26A-2-010. $BaMnF_4$. κ' vs. ν [86Kam]. Parameter: *T*. Curves were obtained from the reflectivity data.

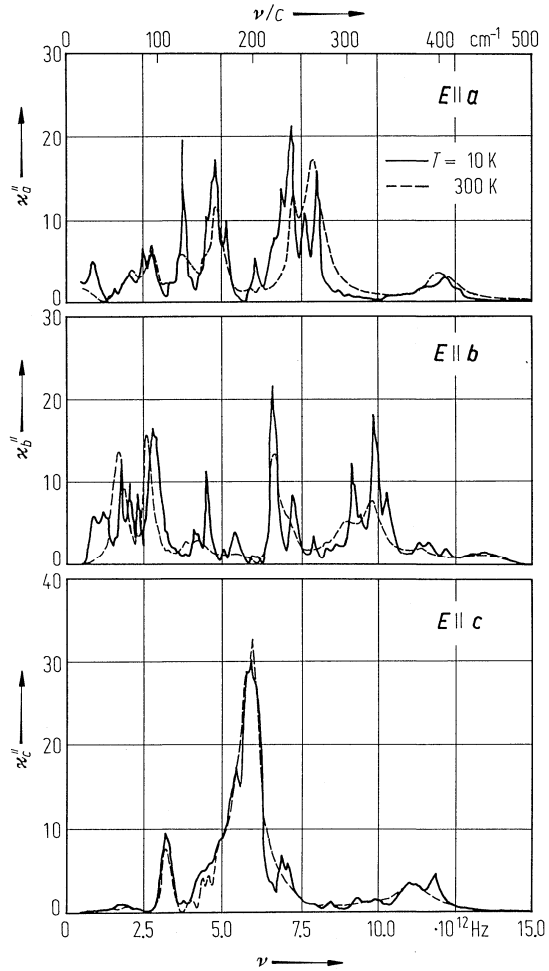

Fig. 26A-2-011. $BaMnF_4$. κ'' vs. ν [86Kam]. Parameter: T. Kramers-Kronig relation was applied for the reflectivity.

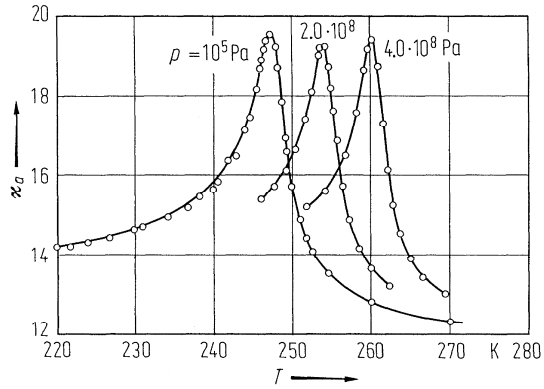

Fig. 26A-2-012. $BaMnF_4$. κ_a vs. T [76Sam]. Parameter: p, hydrostatic pressure. f = 1…100 kHz.

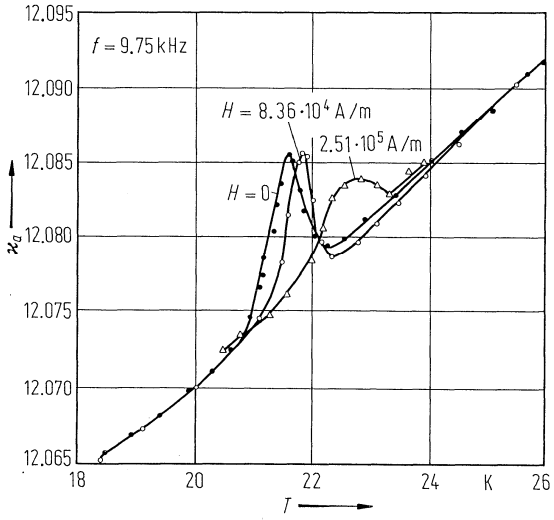

Fig. 26A-2-013. $BaMnF_4$. κ_a vs. T [84Kiz]. Parameter: magnetic field, $\boldsymbol{H}$. $\boldsymbol{H} \parallel b$.

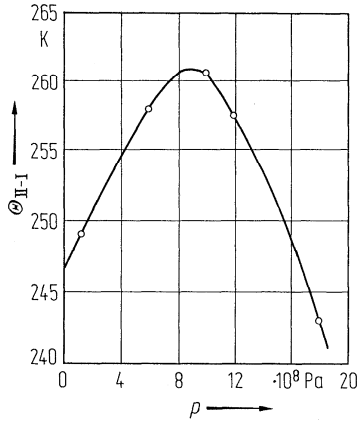

Fig. 26A-2-014. $BaMnF_4$. Θ_{II-I} vs. p [76Sam]. p: quasi-hydrostatic pressure.

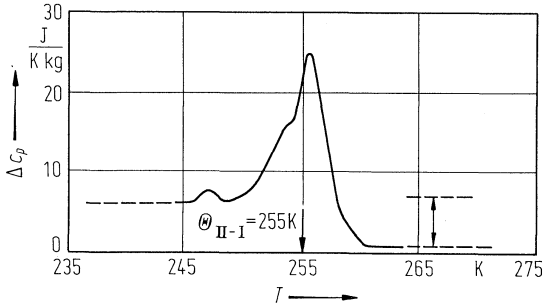

Fig. 26A-2-015. $BaMnF_4$. Δc_p vs. T [82Sco]. Δc_p: change of the specific heat capacity.

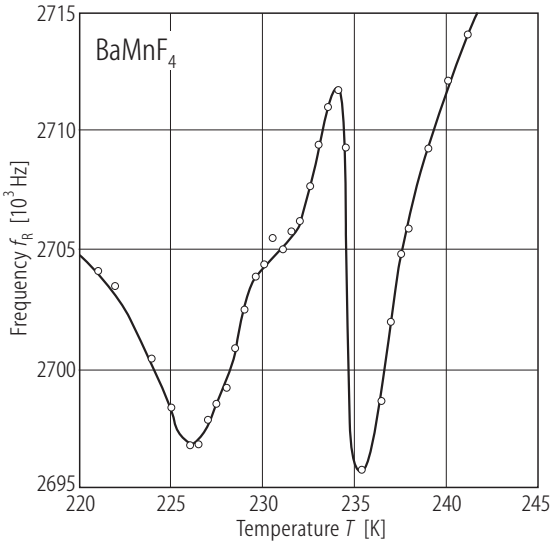

Fig. 26A-2-016. $BaMnF_4$. f_R vs. T [90Hid]. f_R: piezoelectric resonance frequency measured for *b*-plate sample.

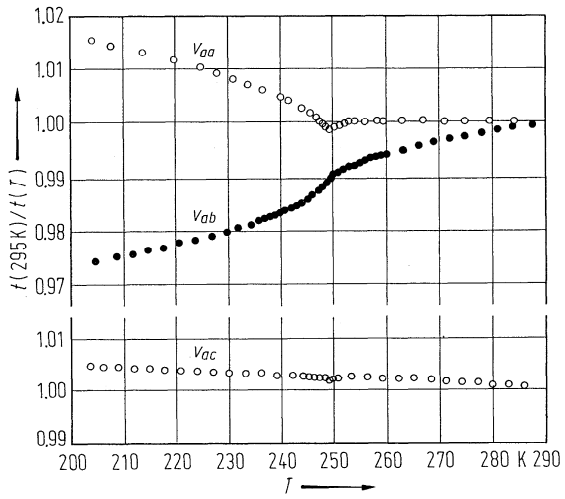

Fig. 26A-2-017. $BaMnF_4$. t(295K)/t(T) vs. T [75Fri]. t: transit time for modes propagating along the *a* axis. f = 30 MHz. t is inversely proportional to the sound velocity. υ_{aa}: longitudinal wave velocity. υ_{ab}: velocity of a sound wave polarized along the *b* axis. υ_{ac}: polarized along the *c* axis.

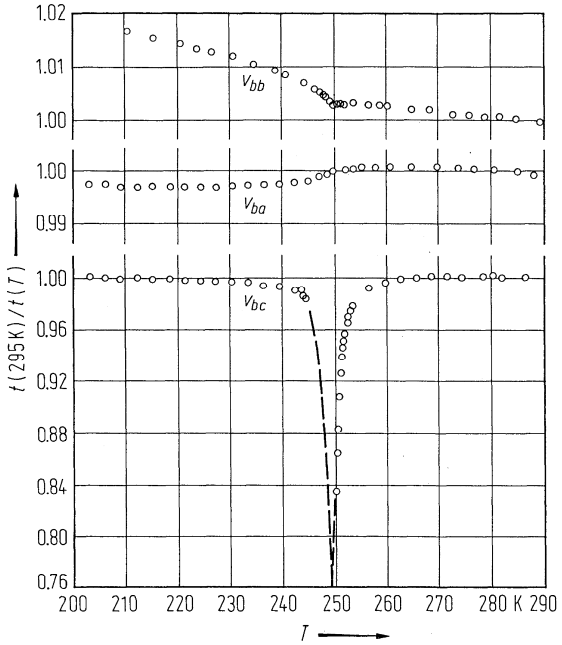

Fig. 26A-2-018. $BaMnF_4$. t(295 K)/$t(T)$ vs. T [75Fri]. t: transit time for modes propagating along the b axis. t is inversely proportional to the sound velocity. Circles: f = 30 MHz. Dashed line: 4 MHz.

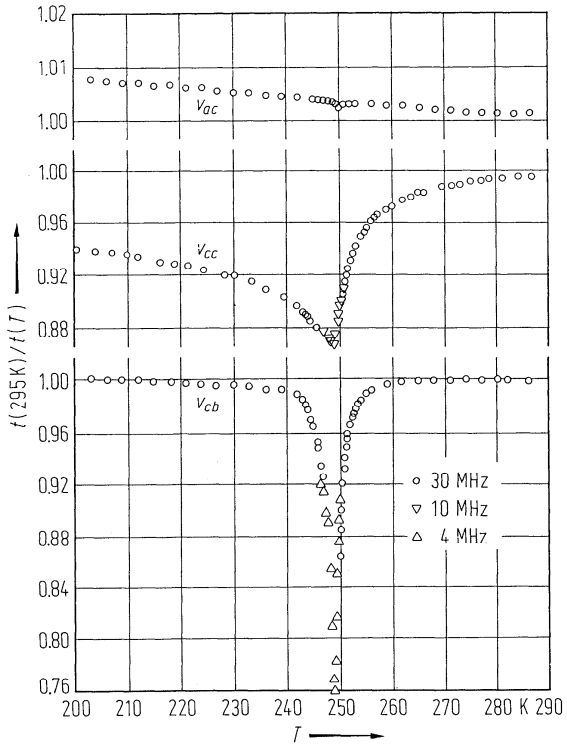

Fig. 26A-2-019. $BaMnF_4$. t(295 K)/$t(T)$ vs. T [75Fri]. t: transit time for modes propagating along the c axis. t is inversely proportional to the sound velocity. Parameter: f.

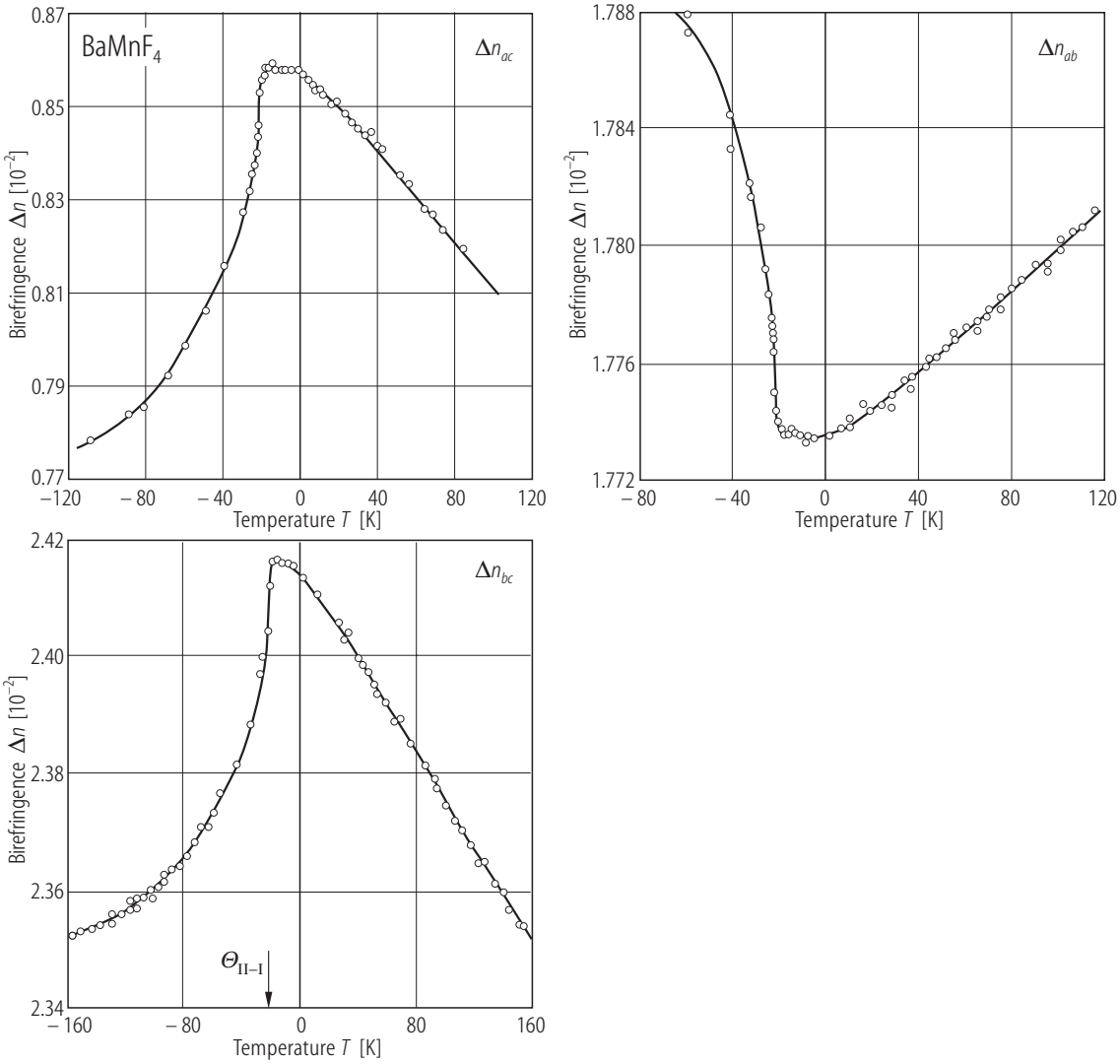

Fig. 26A-2-020. $BaMnF_4$. Δn vs. T [89Asa]. Δn: birefringence.

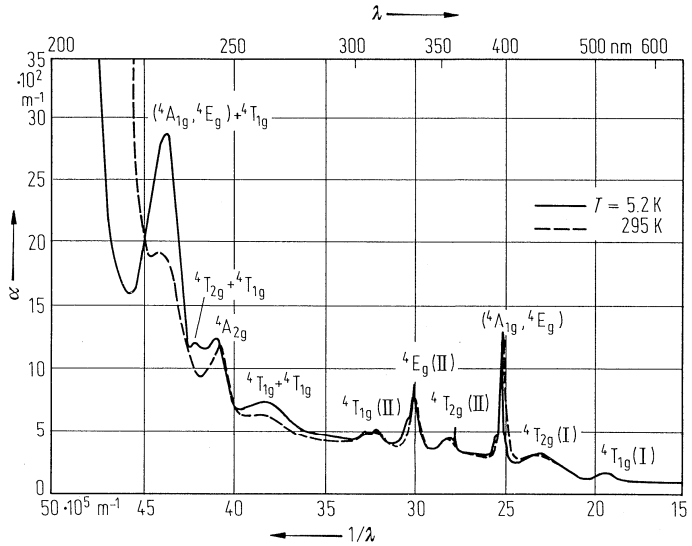

Fig. 26A-2-021. $BaMnF_4$. α vs. $1/\lambda$ [83Tsu]. Parameter: T. α: optical absorption coefficient of unpolarized light on the (*bc*) plane.

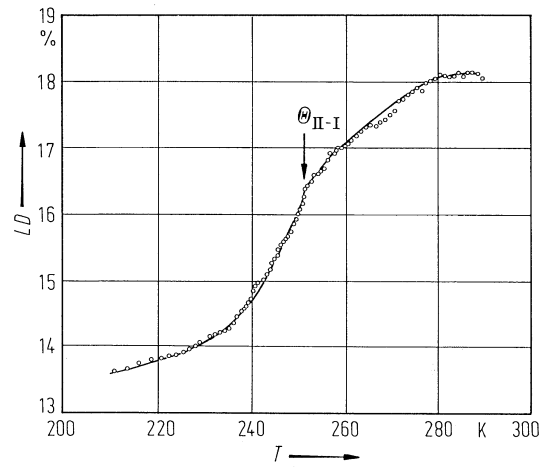

Fig. 26A-2-022. $BaMnF_4$. LD vs. T [80Reg]. LD: linear dichroism $[(\alpha_c - \alpha_a)/(\alpha_c + \alpha_a)]$ in the foot of the $^6A_1(^6S) \rightarrow {}^4A_{1g}, {}^4E_g(^4G)$ transition of Mn^{2+} ions. $\lambda = 398.3$ nm.

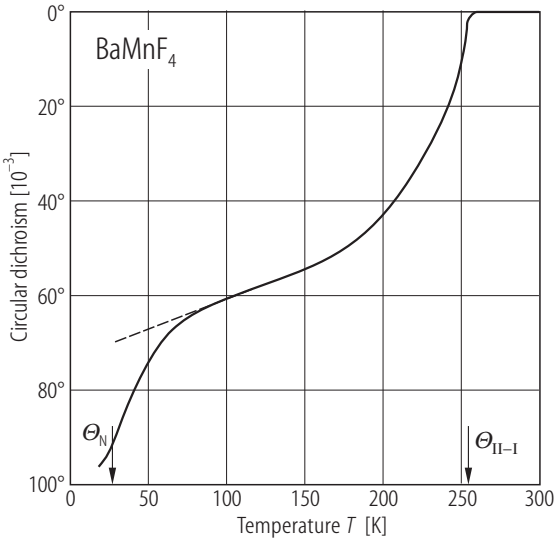

Fig. 26A-2-023. $BaMnF_4$. Circular dichroism of the (*ab*) plate vs. T [85Tsu]. $\lambda = 680$ nm.

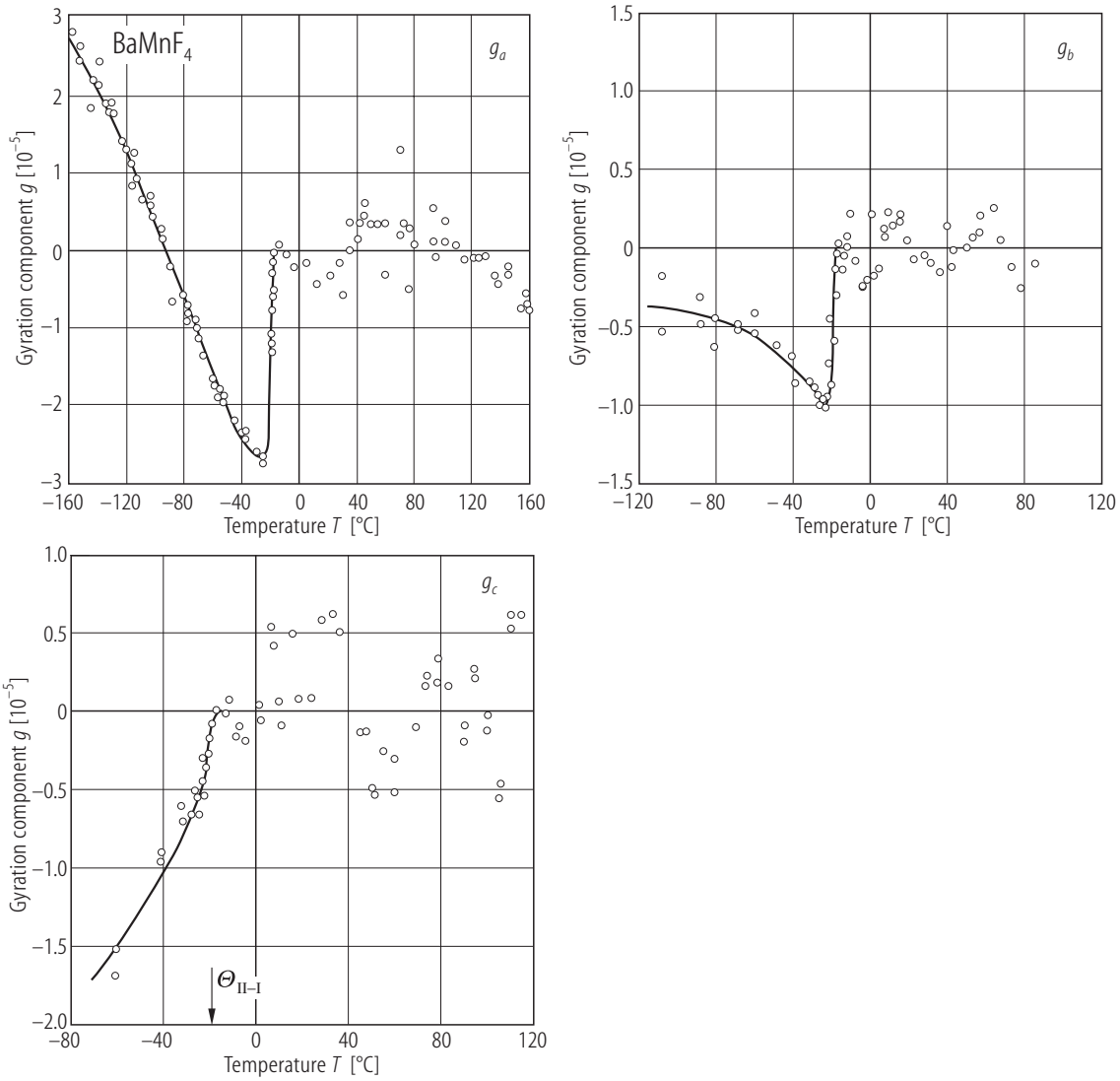

Fig. 26A-2-024. $BaMnF_4$. g_a, g_b, g_c vs. T [89Asa]. g_a, g_b, g_c: gyration for optical activity along the orthorhombic axes [100], [010], and [001], respectively.

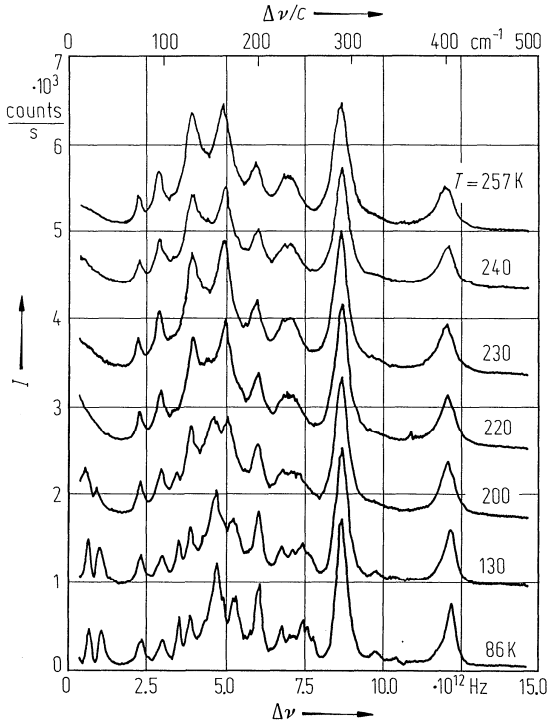

Fig. 26A-2-025. $BaMnF_4$. I vs. $\Delta\nu$ [81Loc]. I: Raman intensity, $\Delta\nu$: Raman shift in the scattering geometry $c(bb)a$. Parameter: T.

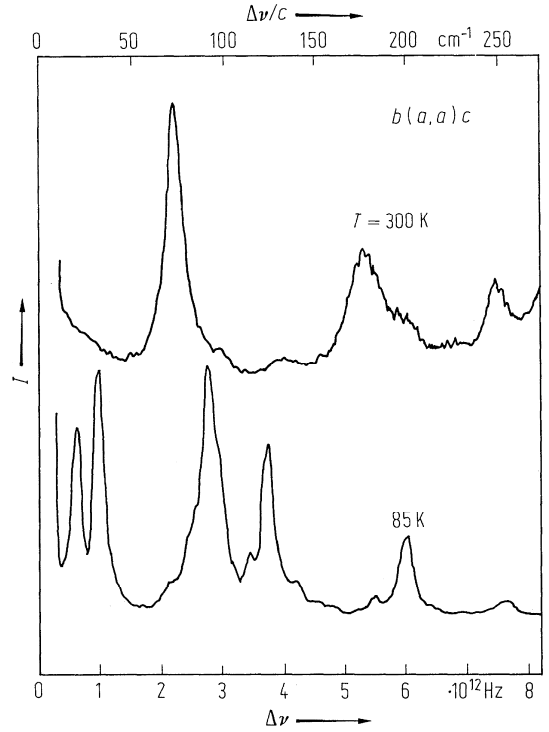

Fig. 26A-2-026. $BaMnF_4$. I vs. $\Delta\nu$ [76Rya]. I: Raman scattering intensity for the scattering geometry of $b(aa)c$ at 300 K (phase I) and at 80 K (phase II).

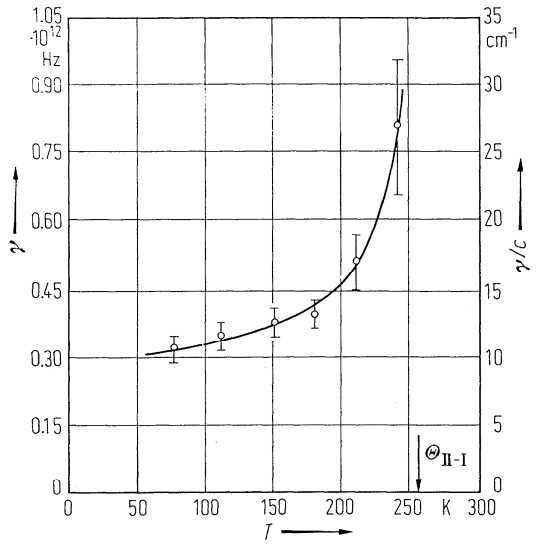

Fig. 26A-2-027. $BaMnF_4$. γ vs. T [76Rya]. γ: damping constant of the soft mode obtained as the full width at half-maximum of the Raman spectrum.

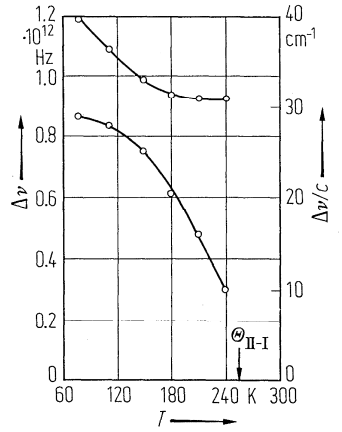

Fig. 26A-2-028. $BaMnF_4$. $\Delta\nu$ vs. T [76Rya]. $\Delta\nu$: Raman frequency shift of the soft mode below $\Theta_{II-I} = 255$ K. For the temperature range of 210 K < T < Θ_{II-I}, the mode is over-damped. See also [74Rya].

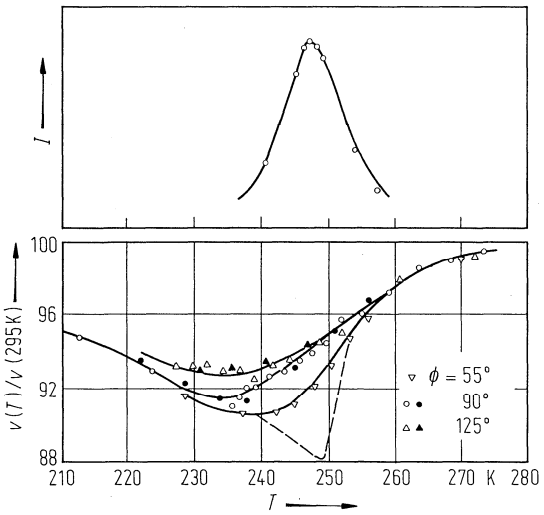

Fig. 26A-2-029. $BaMnF_4$. I vs. T, $\upsilon(T)/\upsilon(295\ \mathrm{K})$ vs. T [82Lyo]. I: intensity of central peak, $\boldsymbol{q} \parallel c$. $\upsilon(T)/\upsilon(295\ \mathrm{K})$: velocity of the longitudinal acoustic wave propagating along c (normalized by the velocity at 295 K). ϕ: scattering angle. The dashed line shows the ultrasonic results [75Fri].

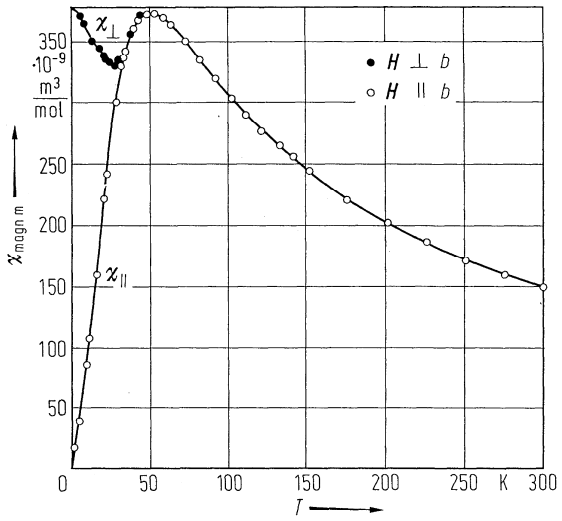

Fig. 26A-2-030. $BaMnF_4$. $\chi_{\mathrm{magn\ m}}$ vs. T [69Hol]. $\chi_\perp$ and $\chi_\parallel$ are the susceptibilities measured perpendicular and parallel to the b axis, respectively.

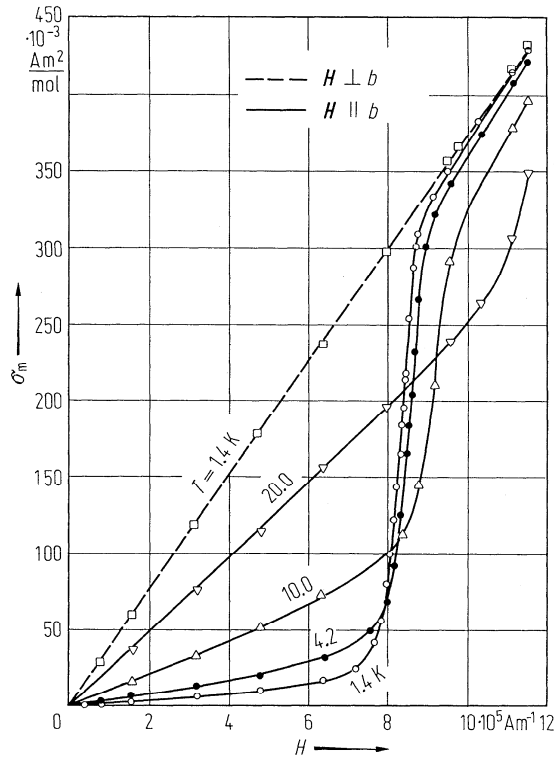

Fig. 26A-2-031. $BaMnF_4$. σ_m vs. H [69Hol]. Parameter: T and field directions, the field is along the b axis except the case (dashed curve) where the field is perpendicular to b.

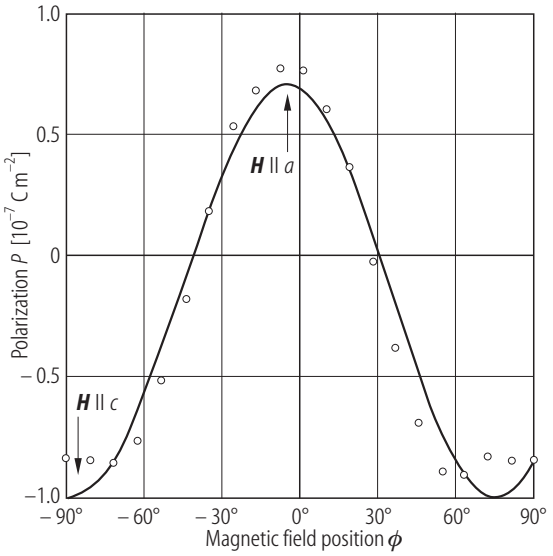

Fig. 26A-2-032. $BaMnF_4$. P vs. ϕ [90Sci]. P: polarization induced by magnetic field. ϕ: angle between magnetic field and a axis in the ac plane. $H = 8 \cdot 10^5$ A m^{-1}. $T = 4$ K.

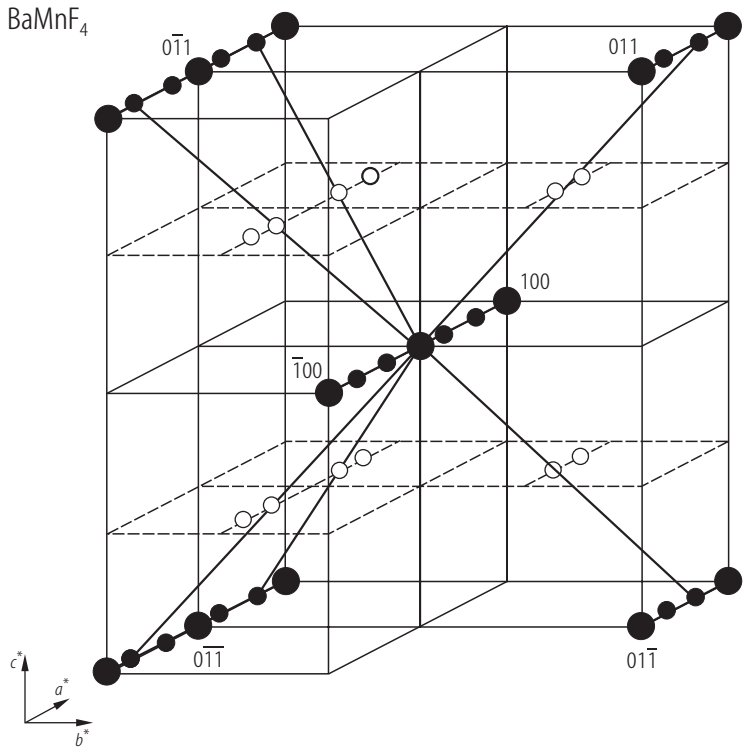

Fig. 26A-2-033. $BaMnF_4$. Main and satellite reflection pattern in phase II [88Sci]. Large full circle: main reflections, open circle: first-order satellite reflections, small full circle: second-order satellite reflections.

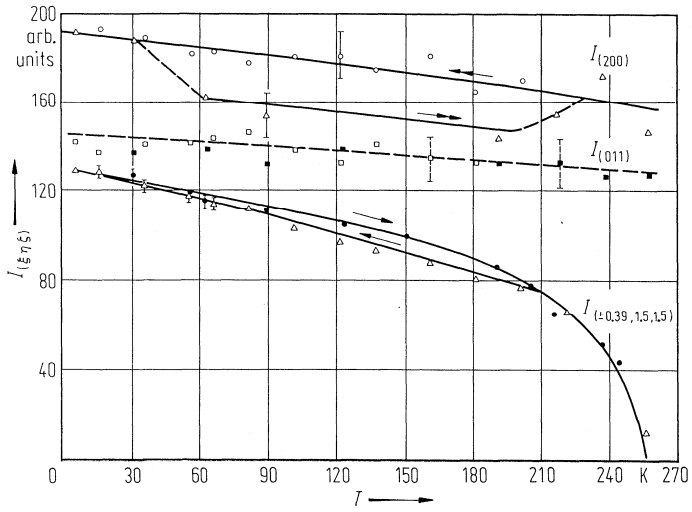

Fig. 26A-2-034. $BaMnF_4$. $I_{(200)}$, $I_{(011)}$, $I_{(\pm 0.39,\ 1.5,\ 1.5)}$ vs. T [83Bar]. $I_{(\xi\eta\zeta)}$: neutron intensity of $(\xi\eta\zeta)$ reflection.

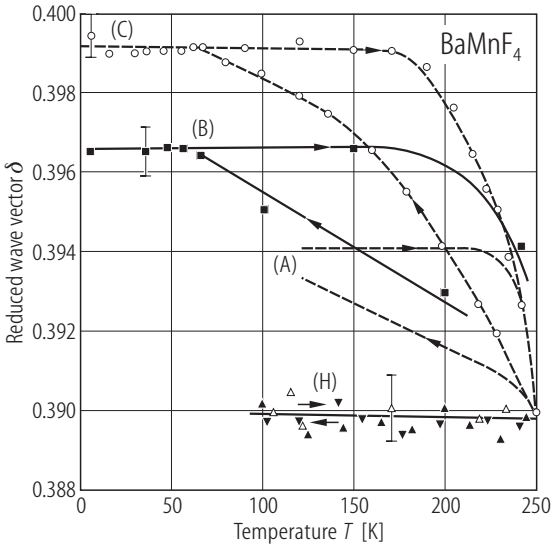

Fig. 26A-2-035. $BaMnF_4$. δ vs. T for four different samples [88StG]. δ: reduced wave vector of satellite reflection at (δ,1/2,1/2). Crystal (A): zone melt growth [83Cox], (B): Bridgman growth [83Bar], (C): Czochralski growth [83Bar], (H): hydrothermal growth.

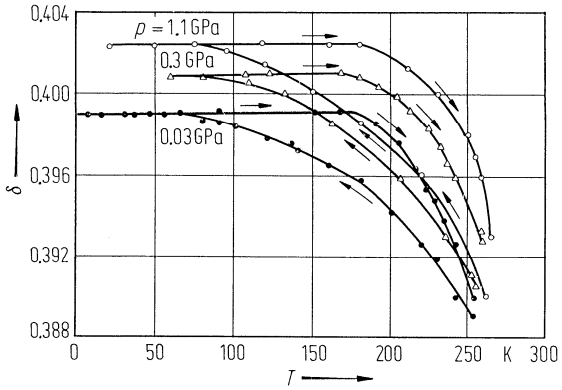

Fig. 26A-2-036. $BaMnF_4$. δ vs. T [84StG]. δ: reduced wave vector of satellite reflection at (δ,1/2,1/2). Parameter: p. Czochralski growth crystal was used.